Analysis of atomic orbital basis sets from the projection of plane-wave results

1996 J. Phys.: Condens. Matter 8 3859

(http://iopscience.iop.org/0953-8984/8/21/012)

J. Phys.: Condens. Matter **8** (1996) 3859–3880. Printed in the UK

Analysis of atomic orbital basis sets from the projection of plane-wave results

Daniel Sánchez-Portal, Emilio Artacho and José M Soler

Instituto de Ciencia de Materiales Nicolás Cabrera and Departamento de Física de la Materia Condensada, C-III, Universidad Autónoma de Madrid, 28049 Madrid, Spain

Received 26 January 1996, in final form 25 March 1996

Abstract. The projection of the eigenfunctions obtained in standard plane-wave first-principles calculations is used for analysing atomic orbital basis sets. The 'spillage' defining the error in such a projection allows the evaluation of the quality of an atomic orbital basis set for a given system and its systematic variational optimization. The spillage is shown to correlate with the mean square error in the energy bands obtained from the projected Hamiltonian matrix. The method is applied to the characterization of finite-range pseudo-atomic orbitals (Sankey O F and Niklewski D J 1989 *Phys. Rev.* B **40** 3979) in comparison to infinite-range pseudo-atomic and Slater-type orbitals. The bases are evaluated and optimized for several zinc-blende semiconductors and for aluminium; the finite-range orbitals display high quality in spite of the limited range. A simple scheme is proposed to systematically enlarge the basis without increasing its range.

1. Introduction

One of the several approximations needed for electronic structure calculations of solids is the truncation of the one-particle Hilbert space. Choosing an appropriate basis is critical for obtaining high-quality results. There are schemes based on localized, extended, or mixed bases. Most of the methods of the first group use atomic-like bases, the eigenfunctions being obtained as linear combinations of atomic orbitals (LCAO methods) [1]. The most widely used among the extended bases is the plane-wave basis [2].

Plane waves (PW) together with pseudopotentials have been shown to offer a very successful calculation scheme for a very large number of applications. Particularly since the development of *ab initio* pseudopotentials [3], PW have provided a tool for very accurate calculation of different properties of solids [2]. PW methods are quite simple to implement and the convergence of the calculations can be controlled with a single parameter, the plane-wave cut-off. The PW basis is also independent of atomic positions, which is very convenient for the coding. However, notwithstanding these advantages, plane waves have important drawbacks, namely (i) the imposed translational invariance (supercells for non-periodic systems), and (ii) their inefficiency as regards basis size.

LCAO methods are much more efficient as regards the size of the required basis. This is a very important advantage for calculations for large systems. Moreover, they have been shown to be very suitable for order-N methods [4] in which the computational effort scales linearly with the size of the system. However, this large reduction in the size of the basis is obviously accompanied by a potential loss of completeness which can affect the results. It is then necessary to choose an appropriate basis to obtain accurate results. Nevertheless, it

0953-8984/96/213859+22$19.50

is important to stress that, once a high-quality atomic basis set has been chosen, calculations can be performed with an accuracy perfectly comparable to that for plane waves, and with a large reduction of CPU time and memory.

Several methods have been developed to optimize LCAO basis sets. Most of them are based on two procedures: (i) minimization of total energies of atoms, molecules, or solids [5]; and (ii) minimization of differences in the energy bands compared with the experiment or with PW calculations [1, 6]. We present here a projection method that links PW and LCAO schemes and provides: (i) a systematic way to characterize the quality of an atomic basis and therefore a way to optimize it; (ii) LCAO energy bands, Hamiltonian and overlap matrix elements; and (iii) chemical information through population analysis. The key of the optimization method is to measure the ability of a set of atomic orbitals to represent the actual eigenstates of the PW calculation of a system. By minimizing the error in the projection of the eigenstates the atomic basis can be optimized for that particular system. This scheme is related to methods of quantum chemistry where a relatively small LCAO basis set is optimized by minimizing the distance (maximizing the overlap) of its subspace to the one spanned by another, larger LCAO basis [7, 8]. The scheme used in this paper was already outlined in [9], the projection technique for bands being already sketched by Chadi in [6].

Besides the projection optimization, the possibility of calculating LCAO band structures and matrix elements allows the characterization of (i) the energies, and (ii) the range of interactions of the basis. Particularly for this purpose, non-orthogonalized atomic basis sets are more adequate, since the interaction parameters have proved to be much more transferable and to have shorter range than for orthogonal bases [10, 11]. The direct use of atomic orbitals in condensed systems gives non-orthogonal basis sets naturally. These non-orthogonal atomic basis sets will be used throughout this paper [12].

In the present paper, this method of analysis and optimization is applied to the characterization of basis sets made up of the finite-range pseudo-atomic orbitals introduced by Sankey and Niklewski [13]. They are compared with the infinite-range pseudo-atomic orbitals [14] and Slater-type orbitals. Both minimal and expanded bases are explored as applied to several zinc-blende semiconductors, as well as to aluminium.

The optimized basis can be used for the calculation of larger systems, where plane-wave calculations are impractical. Besides that possible use, they can also be used directly for the analysis of the PW results themselves [9]. The chemical language of population analysis is not accessible to the PW scheme. The projection into the optimum LCAO basis allows its application, to compute atomic charges, bond charges, and charge transfers. In a similar way to in the decomposition of the total charge into orbital populations, the density of states can also be projected into atomic orbitals to give local densities of states. It is shown here how the optimization of the basis is important for obtaining sensible values of the charges, and also how the projection can be used to partially control the intrinsic arbitrariness of any population analysis.

The structure of this paper is as follows. A brief description of the method for characterizing and optimizing the atomic basis is given in section 2, as well as a description of the way of performing the population analysis and the band-structure calculations. Section 3 describes the main characteristics of the *ab initio* PW calculations used here. A description of the different types of atomic orbital analysed in this paper can be found in section 4. Section 5 proposes the spillage as a parameter to characterize basis sets and their correlations with other quantities. Section 6 contains the results of the analysis and optimization of the different sets of atomic orbitals. Population analysis is discussed in section 7. We end with the conclusions in section 8.

2. Description of the method

The method presented in this paper is based on projection techniques [6, 9]. Given the results of a PW calculation, the projection of the calculated eigenstates onto an atomic basis can provide information about this basis set and about the PW results. A good basis must be able to represent the essential features of the PW eigenstates. Once the PW calculation has been performed for the system of interest, the projection process is much less costly than the self-consistent calculation itself, and many different basis sets can be analysed and optimized for one single PW calculation, a much more economical procedure than performing a full self-consistent calculation for each trial basis set.

On the basis of our method we have the definition of the *spillage* [9]. Given a PW calculation we define the spillage $\mathcal{S}_\Omega$ for a given local basis set as

$$\mathcal{S}_\Omega = \frac{1}{N_k}\frac{1}{N_\alpha}\sum_{k}^{N_k}\sum_{\alpha=1}^{N_\alpha}\langle\psi_\alpha(\boldsymbol{k})|(1-P(\boldsymbol{k}))|\psi_\alpha(\boldsymbol{k})\rangle \tag{1}$$

where $|\psi_\alpha(\boldsymbol{k})\rangle$ are the PW calculated eigenstates, and N_k and N_α are the numbers of calculated $\boldsymbol{k}$-points in the Brillouin zone and the number of bands considered, respectively, and $\mathcal{S}_\Omega$ is the specific subspace spanned by the eigenstates included in the sum (defined by N_k and N_α). $P(\boldsymbol{k})$ is the projector operator for projection into the subspace of Bloch functions of wave vector $\boldsymbol{k}$, generated by the atomic basis, and defined as usual for a non-orthogonal basis [12]:

$$P(\boldsymbol{k}) = \sum_{\mu}|\phi_\mu(\boldsymbol{k})\rangle\langle\phi^\mu(\boldsymbol{k})| = \sum_{\mu\nu}|\phi_\mu(\boldsymbol{k})\rangle S^{-1}_{\mu\nu}(\boldsymbol{k})\langle\phi_\nu(\boldsymbol{k})| \tag{2}$$

where

$$\langle\boldsymbol{r}|\phi_\mu(\boldsymbol{k})\rangle = \sum_{\boldsymbol{R}}\phi_\mu(\boldsymbol{r}-\boldsymbol{r}_\mu-\boldsymbol{R})\mathrm{e}^{\mathrm{i}\boldsymbol{k}\cdot(\boldsymbol{r}_\mu+\boldsymbol{R})} \tag{3}$$

where the $\phi_\mu(\boldsymbol{r})$ are the atomic orbitals, $\boldsymbol{r}_\mu$ the atomic coordinates in the unit cell, and $\boldsymbol{R}$ the lattice vectors.

$$S_{\mu\nu}(\boldsymbol{k}) = \langle\phi_\mu(\boldsymbol{k})|\phi_\nu(\boldsymbol{k})\rangle \tag{4}$$

is the overlap matrix of the atomic basis. The vectors $|\phi^\mu(\boldsymbol{k})\rangle$ constitute the dual of the atomic basis, and satisfy

$$\langle\phi^\mu(\boldsymbol{k})|\phi_\nu(\boldsymbol{k})\rangle = \langle\phi_\mu(\boldsymbol{k})|\phi^\nu(\boldsymbol{k})\rangle = \delta_{\mu\nu}. \tag{5}$$

$\mathcal{S}_\Omega$ is a parameter that varies between 0 and 1 and measures the ability of a basis to represent PW eigenstates, by measuring how much of the subspace of the Hamiltonian eigenstates falls outside the subspace spanned by the atomic basis. If we consider the PW eigenfunctions $|\psi_\alpha(\boldsymbol{k})\rangle$ and their projection onto the atomic basis $P(\boldsymbol{k})|\psi_\alpha(\boldsymbol{k})\rangle$, then $\mathcal{S}_\Omega$ gives the average of $||(1-P)|\psi_\alpha(\boldsymbol{k})\rangle||^2$ over the eigenstates considered for the projection. It must be also pointed out that the projected eigenstates $|\chi_\alpha(\boldsymbol{k})\rangle = P(\boldsymbol{k})|\psi_\alpha(\boldsymbol{k})\rangle$ are not necessarily orthonormal, the overlap matrix $R_{\alpha\beta}(\boldsymbol{k}) = \langle\chi_\alpha(\boldsymbol{k})|\chi_\beta(\boldsymbol{k})\rangle$ being different from the identity matrix. In particular $R_{\alpha\alpha}(\boldsymbol{k}) \leqslant 1$, and

$$\mathcal{S}_\Omega = \frac{1}{N_k}\frac{1}{N_\alpha}\sum_{k}^{N_k}\sum_{\alpha=1}^{N_\alpha}(1-R_{\alpha\alpha}(\boldsymbol{k})) \tag{6}$$

is the averaged norm which has been lost (spilled) in the projection process. If we restrict our analysis to the *occupied* eigenstates, then $\mathcal{S}_\Omega$ is the fraction of total electronic charge spilled when projecting, and will be referred to as *charge spillage* $\mathcal{S}_Q$.

A local spillage can also be defined as a function of real-space coordinates:

$$\mathcal{S}_\Omega(\boldsymbol{r}) = \frac{1}{N_k}\frac{1}{N_\alpha}\sum_{k}^{N_k}\sum_{\alpha=1}^{N_\alpha}(|\psi_\alpha(\boldsymbol{k},\boldsymbol{r})|^2 - |\chi_\alpha(\boldsymbol{k},\boldsymbol{r})|^2). \tag{7}$$

We consider it a useful and direct way for visually characterizing the quality of the representation of the PW eigenstates. The total spillage defined above is recovered by integrating the local spillage over the three-dimensional space.

Important for the characterization of the quality of a basis for a given system is the energy band structure. To calculate the LCAO energy bands of a system we project the Hamiltonian associated with the self-consistent PW charge density of our reference calculation onto the basis subspace:

$$H_{\mu\nu}^{LCAO}(\boldsymbol{k}) = \langle\phi_\mu(\boldsymbol{k})|H^{PW}|\phi_\nu(\boldsymbol{k})\rangle. \tag{8}$$

To obtain the LCAO Hamiltonian matrix elements we expand the Bloch basis functions into plane waves [6]. We calculate the kinetic energy and the effect of the non-local part of the pseudopotential directly in Fourier space. The effect of the local part of the potential and self-consistent Hartree and LDA interactions is calculated using fast Fourier transform algorithms:

$$H_{\mu\nu}^{LCAO}(\boldsymbol{k}) = \sum_{|\boldsymbol{k}+\boldsymbol{G}|^2<E_{max}}\langle\phi_\mu(\boldsymbol{k})|\boldsymbol{k}+\boldsymbol{G}\rangle\langle\boldsymbol{k}+\boldsymbol{G}|H^{PW}|\phi_\nu(\boldsymbol{k})\rangle \tag{9}$$

$$S_{\mu\nu}^{LCAO}(\boldsymbol{k}) = \sum_{|\boldsymbol{k}+\boldsymbol{G}|^2<E_{max}}\langle\phi_\mu(\boldsymbol{k})|\boldsymbol{k}+\boldsymbol{G}\rangle\langle\boldsymbol{k}+\boldsymbol{G}|\phi_\nu(\boldsymbol{k})\rangle \tag{10}$$

where the $\boldsymbol{G}$ are reciprocal-lattice vectors and E_{max} is an energy cut-off independent of the one used in the PW calculation, which must be large enough to guarantee a reliable representation of the atomic basis. With this method we obtain a LCAO Hamiltonian from a first-principles PW calculation, no free parameters being fitted.

The LCAO Hamiltonian is obtained in Bloch space and, as a consequence, it includes interactions up to infinite neighbours. The deviations in the band structure with respect to the PW only reflect the incompleteness and inadequacy of the basis, clearly separated from the possible additional approximation of neglecting matrix elements beyond some range of interactions. We can study the two approximations separately. In most studies of LCAO band structures these two effects are mixed together. As an exception we must mention the work of Chadi [6] and of Jansen and Sankey [14], where LCAO Hamiltonians with interactions up to an infinite range of neighbours are also obtained.

The Hamiltonian matrix in real space is calculated from the Hamiltonian matrix in Bloch space by performing a Bloch-type transformation:

$$H_{\mu\nu}^{LCAO}(\boldsymbol{R}_{\mu\nu}) = \sum_{\boldsymbol{k}} H_{\mu\nu}^{LCAO}(\boldsymbol{k})\mathrm{e}^{\mathrm{i}\boldsymbol{k}\cdot(\boldsymbol{R}_\mu-\boldsymbol{R}_\nu)} \tag{11}$$

$$S_{\mu\nu}^{LCAO}(\boldsymbol{R}_{\mu\nu}) = \sum_{\boldsymbol{k}} S_{\mu\nu}^{LCAO}(\boldsymbol{k})\mathrm{e}^{\mathrm{i}\boldsymbol{k}\cdot(\boldsymbol{R}_\mu-\boldsymbol{R}_\nu)} \tag{12}$$

where normalization factors which depend on the overlaps are omitted for clarity. The sum has to be extended to a sufficient number of $\boldsymbol{k}$-points, taking into account that the number of points depends on the real-space range of the interactions [15, 16].

The projection technique can also be used for obtaining chemical information from the PW calculations by means of an LCAO population analysis. We use the one proposed by Mulliken [17]. The PW occupied eigenstates are projected onto the subspace spanned by

the atomic basis. Due to the non-orthogonality of the projected eigenstates, the density operator has to be properly defined to ensure charge conservation:

$$\hat{\rho} = \sum_{\boldsymbol{k}} \sum_{\alpha}^{occ} |\chi_\alpha(\boldsymbol{k})\rangle\langle\chi^\alpha(\boldsymbol{k})| \tag{13}$$

where

$$|\chi^\alpha(\boldsymbol{k})\rangle = \sum_{\beta} R^{-1}_{\beta\alpha}(\boldsymbol{k})|\chi_\beta(\boldsymbol{k})\rangle$$

represent the vectors of the dual set of the projected eigenstates, and $R_{\beta\alpha}(\boldsymbol{k}) = \langle\chi_\beta(\boldsymbol{k})|\chi_\alpha(\boldsymbol{k})\rangle$. The LCAO density matrix is then written in terms of the dual LCAO basis:

$$\mathcal{P}_{\mu\nu} = \langle\phi^\mu|\hat{\rho}|\phi^\nu\rangle \tag{14}$$

where the charge associated with an orbital μ is

$$Q_\mu = \sum_{\nu} \mathcal{P}_{\mu\nu} S_{\nu\mu}. \tag{15}$$

3. Reference calculations

The analyses of the bases presented in this paper are based on reference PW calculations which have been performed using *ab initio* pseudopotentials generated by the improved Troullier–Martins method [18] and within the local density approximation (LDA) for electron exchange and correlation [19]. Of course, other schemes could have equally been used, the only requirement for applying the method being the plane-wave expansion of the one-electron wave-functions. The energy cut-off for the plane-wave expansion has been taken large enough to allow us to consider that all of the calculations are well converged. High-energy cut-offs are not necessary for the application of the method but are important to ensure accurate results for the optimization of the orbitals as well as for the population analysis. The cut-offs used are: 10 Ryd for Al; 20 Ryd for Si, BP, and AlP; 30 Ryd for GaAs; 40 Ryd for graphite; 50 Ryd for BN; and 70 Ryd for C and SiC. For the self-consistent zinc-blende semiconductor calculations, we used two irreducible-Brillouin-zone points (IBZP), equivalent to 32 whole-Brillouin-zone points (BZP), giving a k-mesh *length cut-off* [16] $l_c = a$, where a is the lattice constant. For aluminium and graphite we used, respectively, 10 IBZP, 125 BZP, $l_c = 13.435$ au, and 8 IBZP, 16 BZP, $l_c = 4.648$ au. The length cut-off l_c is simply related to the maximum range of the real-space matrix elements obtainable from the PW calculation (equations (11) and (12)) by $|\boldsymbol{R}_{\mu\nu}| < l_c$. For the pseudopotentials, in all of the calculations we have used the separable, fully non-local formulation following Kleinman and Bylander [20].

4. Atomic basis sets

A brief description follows of the sets of atomic orbitals which are used throughout this work. The basis sets studied can be classified into two groups: (i) those which are provided by the numerical solution of the atomic problem (with the same atomic pseudopotential as used in the PW calculation), hereafter called PAO (for pseudo-atomic orbitals) [13, 14]; and (ii) Slater-type orbitals (STO) [5].

Within the first group, PAO_∞ are the atomic solutions under real atomic boundary conditions (at $r = \infty$). This family of bases allows for a scaling factor for the radial

part acting as a variational parameter to optimize the atomic orbitals via the spillage minimization:

$$\phi_l^{opt}(\boldsymbol{r}) = \lambda_l^{3/2}\phi_l^{atm}(\lambda_l \boldsymbol{r}). \tag{16}$$

PAO_∞ represents quite a natural choice, since access to PW calculations is usually accompanied by access to atomic calculations under the same approximations. They provide a good description of the charge density and have already been used in *ab initio* calculations [14] giving accurate results. For covalent materials, with small charge transfers, they provide a very good description of the pseudo-core region. This is worth considering since the PW eigenstates are expanded in the atomic basis maximizing the projection without making any distinction between the pseudo-core region (the zone near the atomic nucleus) and the valence region (the interatomic zone).

The main disadvantage of the PAO_∞ is the very long range of the interactions and overlaps that they originate. Getting a shorter and perfectly defined range of interactions is the reason to work with PAO_{r_c}. They are the solutions of the atomic pseudopotential when forced to vanish outside a cut-off radius r_c, keeping the continuity, as introduced by Sankey and Niklewski [13] (they will be denoted by specifying the value of r_c in atomic units). The cut-off radius represents a variational parameter for this type of basis. These orbitals seem promising candidates in calculation techniques for very large systems [4].

Within the Slater orbitals, we use the name STO1 for the conventional orbitals $r^{n-1}\exp^{(-\beta r)}$, where n is the principal quantum number and the scale factor β is taken to be the same for all of the atomic orbitals within the same shell; STO2 will be the same, but allowing for a different β for each orbital, $\beta_s \neq \beta_p \neq \beta_d$; and STO3 are the orbitals $r^\alpha \exp^{(-\beta r)}$, where α becomes another variational parameter, no longer restricted to being an integer, and allowing both α and β to be different for each orbital.

STO have been extensively used in LCAO calculations in quantum chemistry and have proven to provide accurate results [5]. They present the additional advantage of their very simple mathematical properties. To simplify the computational task, it is a common practice to expand the STO orbitals as linear combinations of gaussian functions. These are the so-called STO-NG [5] orbitals where N stands for the number of gaussian orbitals used per STO. We have made some tests to compare the results obtained using STO and STO-4G orbitals. No appreciable differences have been found in the results. Spillage values and optimum exponents are essentially the same in the two cases, and no further investigation has been pursued concerning STO-NG orbitals.

STO orbitals do not seem *a priori* to be very well suited for the description of the pseudo-core region for the projection, possibly leading to a worsening of the spillage in the valence region while trying to adapt the pseudo-core. To explore that possibility we consider a last kind of orbital function, the pseudo-STO, which represent a link between the STO and the PAO families. A pseudo-STO is a Slater-type orbital outside a certain radius, and the numerical solution of the pseudopotential inside that radius—continuity of the function and its derivative being imposed.

5. Spillage analysis

This section is devoted to showing the adequacy of an analysis based on the projection and the spillage for the evaluation of a basis set. The total spillage provides a natural parameter that can be used straightforwardly to measure systematically the quality of a basis. The optimization in terms of spillage provides a variational scheme, since the minimum attainable is zero, which means a perfect basis.

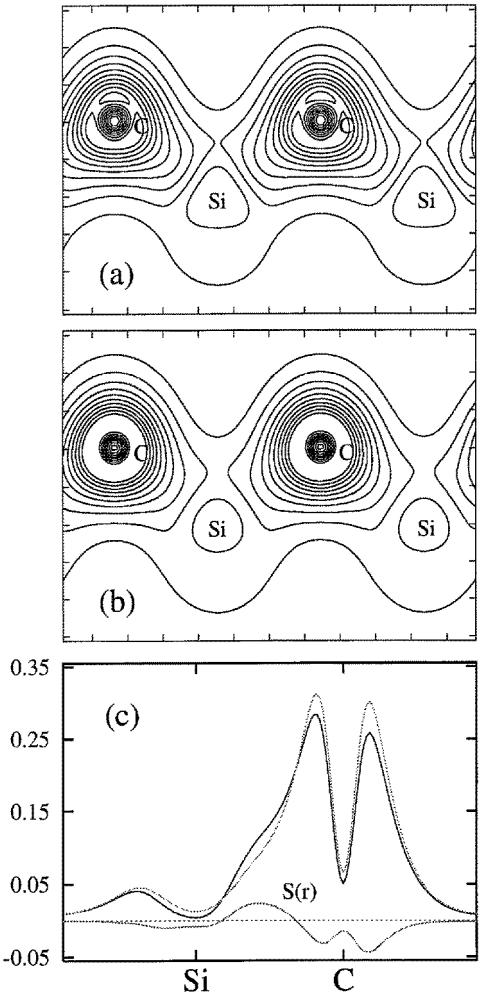

Figure 1. The electron charge density for SiC: (a) the self-consistent density contour map in the (110) plane calculated using PW; (b) the same after projecting the eigenstates onto a PAO_∞ sp basis; and (c) these two densities (PW shown with solid lines and the projected density with dotted lines) and $\mathcal{S}_Q(\boldsymbol{r})$ along the bond axis. The units are electrons per unit cell.

Both the projected charge density and the local spillage offer useful tools for visually characterizing the quality of a basis. This is illustrated in figure 1, where a charge-density contour map for SiC is shown comparing the PW results with the results of the projection on the PAO_∞, showing in addition the local spillage along the bond axis. We see that some of the bond structure is lost, the charge density being much more spherical around the atoms, when projecting on this basis. This can be also seen in the fact that the two maxima in the density near the carbon nucleus are of approximately the same height, while in the PW calculation there is more density on the bond side. All of these features can be seen in the local spillage, which is negative in the regions with an excess of projected charge and positive in the zones with a deficit of projected charge. The local charge spillage is negative in the proximity of both core regions and positive in the bond region. Some of the bond charge goes to an anti-bonding region. This feature also tends to make the charge transfer lower for this PAO_∞ basis (see below).

For the spillage analysis to be useful, the spillage has to be correlated with the quality in the energetics of the system. This is tested in figure 2, where the mean square error of

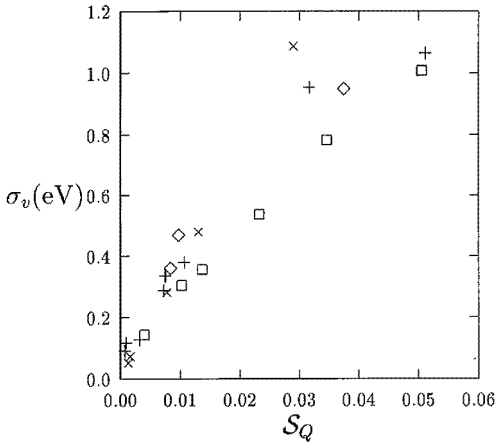

Figure 2. The mean square deviation in valence bands of the projected Hamiltonian from the PW bands versus the charge spillage of different bases in silicon. Each symbol stands for a different family of bases: □ for PAO_{r_c}, × for PAO_∞, + for STO, and ◊ for different double-z bases. Bases with σ_v lower than 0.2 eV include d orbitals.

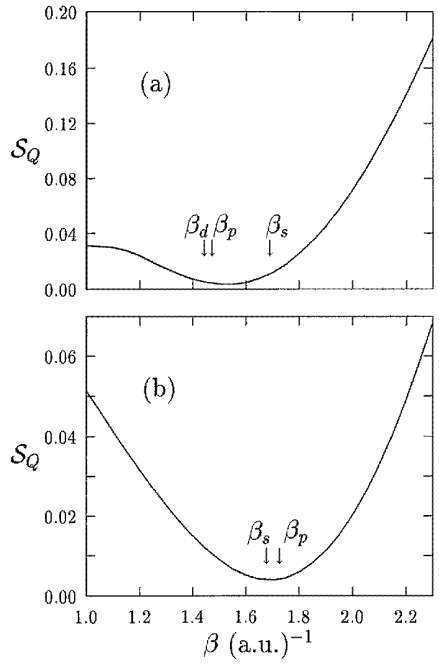

Figure 3. Charge spillage versus the exponent for a STO1 basis set: (a) silicon with an spd basis; and (b) diamond with an sp basis. Also shown are the optimum exponents for a STO2 basis set for the same systems.

the projected valence bands of crystalline silicon, as compared to the PW ones, is plotted versus the charge spillage $\mathcal{S}_Q$, for different families of bases. It is calculated without shifting the bands, the absolute zero being unambiguously defined (the Hamiltonian operator is not

changed). This quantity can also be taken as an indicator of the error in the total energy due to the approximation of the basis.

The clear correlation between the spillage and the error in the energy bands displayed in figure 2 indicates that a basis optimization based on a minimization of the spillage is parallel (at least approximately) to an energy minimization. This parallelism is even clearer within a basis family, where the correlation is much more pronounced (different points within the same family are obtained by varying the characteristic parameters presented above).

To finish this section, we introduce a lower bound for the spillage. The dependence of $\mathcal{S}_\Omega$ on the atomic basis enters through the Fourier coefficients of the radial wave-functions. Therefore, $\mathcal{S}_\Omega$ can be regarded as a function of these Fourier coefficients $\phi_{i,\mu}(|\boldsymbol{k}+\boldsymbol{G}|)$, which are different for each atom i, orbital μ and each modulus $|\boldsymbol{k}+\boldsymbol{G}|$. Considering all of these Fourier coefficients as free variables, the minimization of $\mathcal{S}_\Omega$ gives a lower bound for $\mathcal{S}_\Omega$. Values of this lower bound will be shown as Min $\mathcal{S}$ in the tables.

6. Analysis and optimization of atomic basis sets

The quality of the LCAO bases presented above is measured and optimized for different solids in this section using the spillage analysis, and, simultaneously, the LCAO band structure is contrasted with the results for plane waves. The results are displayed in tables 1 to 4. The resulting numbers are abundant since the number of possibilities is large. For the different kinds of basis introduced in section 4 there are different possible basis sizes, of single-z or double-z type, meaning one or two orbitals per atomic symmetry. There is the additional possibility of polarizing the basis, i.e., introducing atomic orbitals of a higher angular momentum than needed, which, in the cases of this paper, represents the addition of the d orbitals to the minimal sp basis.

The optimization of the different bases introduces new degrees of freedom since their optimization is done with respect to different variational parameters (see section 4), and also the spillage can be defined for different numbers of bands, depending on the particular application for which the basis is optimized.

6.1. Minimal basis sets

Table 1 shows the spillages of the projections onto different minimal bases for silicon, diamond, and aluminium, together with the mean square error in the LCAO bands as compared with the PW ones. Only sp bases are considered, except for for Al, for which also spd-basis data are shown due to the poorness of minimal sp bases for this solid. The numbers displayed for STO bases have been obtained after minimization of the charge spillage (the spillage of the valence eigenvectors) for the corresponding parameters. This procedure is illustrated in figure 3 for the specific cases for silicon and carbon, where the charge spillage is shown as a function of the STO exponents. $\mathrm{PAO}_\infty^{opt}$ stands in table 1 for the PAO_∞ optimized via a scale factor. The PAO_{r_c} are optimized with respect to the radii of the basis functions, r_c, as illustrated in figures 4, 5, and 6 for silicon, diamond, and aluminium, respectively. In table 1, specific values of r_c are chosen.

All of the bases displayed in table 1 perform comparably well as regards the charge spillage. sp is clearly better for C than for Si and Al, as expected, since d orbitals play a lesser role for C than for Si and Al. The spillage for eigenstates including conduction bands is larger than for valence bands only. For sp bases there is a factor of 10 to 20. The two main reasons for that are: (i) the bases have been optimized by minimizing the charge spillage; and (ii) higher-energy bands require higher-energy atomic orbitals.

Table 1. Bases for silicon (sp), diamond (sp), and aluminium (sp and spd). $\mathcal{S}_Q$ stands for the charge spillage, and $\mathcal{S}_4$ and $\mathcal{S}_8$ for the spillage considering the first 4 and 8 bands, respectively. PAO_∞ and PAO_{r_c} are fixed bases, whereas STO1, STO2, STO3, and PAO_∞^{opt} have been optimized according to their respective variational parameters, to minimize $\mathcal{S}_Q$. Q_s, Q_p, and Q_d are the total charges assigned to s, p, and d orbitals. The mean square error of the LCAO bands with respect to the PW reference bands (in eV) is displayed for the valence bands (σ_v) and the first two conduction bands (σ_c) for silicon and diamond, and for the first and second bands (σ_{1+2}) and third and fourth (σ_{3+4}) for aluminium. Min $\mathcal{S}$ corresponds to the spillage lower bound (see the text).

	Basis		$\mathcal{S}_Q$	$\mathcal{S}_8$	Q_s	Q_p		σ_v	σ_c
Si	PAO_∞	sp	0.0080	0.1596	1.32	2.68		0.30	2.15
	PAO_∞^{opt}	sp	0.0078	0.1621	1.35	2.65		0.29	1.97
	$PAO_{5.0}$	sp	0.0139	0.1591	1.40	2.60		0.36	2.09
	STO1	sp	0.0109	0.1764	1.48	2.52		0.38	2.43
	STO2	sp	0.0076	0.1562	1.36	2.64		0.34	2.34
	STO3	sp	0.0074	0.1548	1.34	2.66		0.29	1.95
	Min $\mathcal{S}$	sp	0.0044	0.0689					
	Min $\mathcal{S}$	spd	0.0001	0.0014					
	Basis		$\mathcal{S}_Q$	$\mathcal{S}_8$	Q_s	Q_p		σ_v	σ_c
C	PAO_∞	sp	0.0035	0.0719	1.05	2.95		0.32	2.19
	PAO_∞^{opt}	sp	0.0027	0.0780	1.07	2.93		0.25	2.61
	$PAO_{4.0}$	sp	0.0041	0.0672	1.10	2.90		0.23	2.22
	STO1	sp	0.0039	0.0771	1.11	2.89		0.26	3.07
	STO2	sp	0.0039	0.0775	1.12	2.88		0.24	3.05
	STO3	sp	0.0024	0.0790	1.09	2.98		0.17	3.36
	Min $\mathcal{S}$	sp	0.0008	0.0226					
	Basis		$\mathcal{S}_Q$	$\mathcal{S}_4$	Q_s	Q_p	Q_d	σ_{1+2}	σ_{3+4}
Al	PAO_∞	sp	0.0165	0.1141	1.13	2.87		2.03	3.45
	PAO_∞	spd	0.0022	0.0053	0.77	1.39	0.84	0.61	0.24
	PAO_∞^{opt}	spd	0.0011	0.0079	0.98	1.41	0.61	0.35	0.84
	$PAO_{6.0}$	sp	0.0157	0.1012	1.30	1.70		1.54	2.97
	$PAO_{6.0}$	spd	0.0014	0.0042	1.02	1.39	0.59	0.20	0.45
	$PAO_{5.3}$	sp	0.0158	0.0930	1.34	1.66		1.34	2.63
	$PAO_{5.3}$	spd	0.0007	0.0020	1.15	1.45	0.40	0.97	2.15
	Min $\mathcal{S}$	sp	0.0009	0.0025					
	Min $\mathcal{S}$	spd	2.9×10^{-5}	0.0007					

Table 1 also shows the populations of s, p, and d orbitals (if present). It can be seen that the sp^3 hybridization is better accomplished in C than in Si (a perfect hybridization would show $Q_s = 1$ and $Q_p = 3$). Q_d for Al is quite appreciable.

The mean square error in the energy bands is displayed as σ_v for the valence bands and σ_c for the first two conduction bands (σ_{1+2} for first two bands, and σ_{3+4} for third and fourth, in the case of aluminium). The valence bands are quite well described with sp bases for Si and C, but not for Al. The metallicity in Al demands a larger contribution of d orbitals, which makes them necessary for any quantitative LCAO description of Al. The conduction

Table 2. Basis optimizations for different number of bands, for Si, C (diamond), BN, and Al. The superscripts indicate the number of bands used for the $\mathcal{S}$-minimization (v means valence bands). The basis is minimal, except for for Al, for which it is spd. $\mathcal{S}_Q$ is the charge spillage, and $\mathcal{S}_4$ and $\mathcal{S}_8$ are the spillages considering the first 4 and 8 bands, respectively. The mean square error of the LCAO bands with respect to the PW reference bands (in eV) is displayed for the valence bands (σ_v) and the first two conduction bands (σ_c) for Si, C, and BN, and for the first and second bands (σ_{1+2}) and third and fourth (σ_{3+4}) for Al. E^{Γ}_{gap} and E_{gap} are the direct gap at Γ and the absolute gap, respectively, both in eV. $\boldsymbol{k}$ is the wave vector of the minimum of the conduction band in units of π/a, being $|\boldsymbol{k}| = 1$ for the X point.

	Basis	$\mathcal{S}_Q$	$\mathcal{S}_8$	σ_v	σ_c	E^{Γ}_{gap}	E_{gap}	$\lvert\boldsymbol{k}\rvert$
Si	$\mathrm{PAO}^{v}_{\infty}$	0.0078	0.1621	0.28	1.97	2.91	1.69	0.63
	$\mathrm{PAO}^{8}_{\infty}$	0.0348	0.1233	0.94	2.13	2.33	1.44	0.80
	$\mathrm{PAO}^{v}_{5.0}$	0.0136	0.1453	0.44	2.16	2.78	1.96	0.62
	$\mathrm{PAO}^{8}_{5.0}$	0.0230	0.1170	0.91	2.47	2.50	0.95	0.83
	$\mathrm{STO1}^{v}$	0.0109	0.1764	0.38	2.43	2.83	2.60	0.47
	$\mathrm{STO1}^{8}$	0.0207	0.1541	0.60	2.27	2.40	1.94	0.60
	$\mathrm{STO2}^{v}$	0.0076	0.1562	0.34	2.34	2.66	2.09	0.53
	$\mathrm{STO2}^{8}$	0.0306	0.1179	0.79	1.48	2.39	0.85	0.80
	$\mathrm{STO3}^{v}$	0.0074	0.1548	0.29	1.95	2.66	1.74	0.60
	$\mathrm{STO3}^{8}$	0.0465	0.1121	1.20	1.28	2.52	0.53	0.83
	PW					2.55	0.45	0.85
	Basis	$\mathcal{S}_Q$	$\mathcal{S}_8$	σ_v	σ_c	E^{Γ}_{gap}	E_{gap}	$\lvert\boldsymbol{k}\rvert$
C	$\mathrm{PAO}^{v}_{\infty}$	0.0027	0.0780	0.25	2.61	6.57	5.83	0.50
	$\mathrm{PAO}^{8}_{\infty}$	0.0192	0.0600	0.89	2.04	5.19	4.13	0.67
	$\mathrm{STO1}^{v}$	0.0039	0.0771	0.26	3.07	5.78	5.78	0.00
	$\mathrm{STO1}^{8}$	0.0208	0.0592	0.94	1.95	4.67	4.34	0.42
	$\mathrm{STO2}^{v}$	0.0039	0.0775	0.24	3.05	5.79	5.79	0.00
	$\mathrm{STO2}^{8}$	0.0293	0.0545	1.37	1.88	4.49	3.51	0.58
	$\mathrm{STO3}^{v}$	0.0024	0.0790	0.17	3.36	6.32	6.18	0.42
	$\mathrm{STO3}^{8}$	0.0335	0.0526	1.32	1.46	4.81	3.96	0.67
	PW					5.28	3.43	0.76
	Basis	$\mathcal{S}_Q$	$\mathcal{S}_8$	σ_v	σ_c	E^{Γ}_{gap}	E_{gap}	$\lvert\boldsymbol{k}\rvert$
BN	$\mathrm{PAO}^{v}_{\infty}$	0.0022	0.0766	0.24	3.06	10.90	8.56	0.93
	$\mathrm{PAO}^{8}_{\infty}$	0.0154	0.0534	0.96	2.21	7.93	4.63	0.93
	PW					8.19	3.82	0.93
	Basis	$\mathcal{S}_Q$	$\mathcal{S}_4$	σ_{1+2}	σ_{3+4}			
Al	$\mathrm{PAO}^{v}_{\infty}$	0.0011	0.0079	0.35	0.84			
	$\mathrm{PAO}^{4}_{\infty}$	0.0036	0.0024	0.37	0.23			

bands are much less well described by the minimal bases shown in the table.

The dependence in the number of bands to be optimized through the spillage is shown in table 2 for Si, C, BN, and Al. Each kind of basis has been optimized by minimizing (i) the charge spillage and (ii) a spillage including conduction bands ($\mathcal{S}_8$ for Si, C, and BN; and

Table 3. The interaction range for minimal sp bases in Si. NS stands for the number of neighbour shells with non-negligible interactions and $r_{99.9\%}$ is a measure of the size of the orbitals as defined in the text. $\mathcal{S}_Q$ stands for the charge spillage, and $\mathcal{S}_8$ for the spillage considering the first 8 bands. The mean square error of the LCAO bands with respect to the PW reference bands (in eV) is displayed for the valence bands (σ_v) and the first two conduction bands (σ_c). $\mathrm{STO1}_{1.75}$ and $\mathrm{STO1}_{1.85}$ are the STO1 bases for the exponents $\beta = 1.75$ au^{-1} [5] and 1.85, respectively.

Basis	$\mathcal{S}_Q$	$\mathcal{S}_8$	σ_v	σ_c	$r_{99.9\%}$	NS
$\mathrm{STO1}_{1.75}$	0.0319	0.2279	0.96	4.27	5.1	4
$\mathrm{STO1}_{1.85}$	0.0514	0.2533	1.07	4.64	4.8	3
PAO_{∞}	0.0080	0.1596	0.30	2.15	7.9	9
$\mathrm{PAO}_{5.0}$	0.0139	0.1591	0.36	2.09	4.6	3
$\mathrm{PAO}_{4.0}$	0.0506	0.2269	1.01	3.89	3.7	2

Table 4. Single-z, double-z (2-z), and spd bases for Si and C (diamond). $\mathcal{S}_Q$ stands for the charge spillage, and $\mathcal{S}_8$ for the spillage considering the first 8 bands. The mean square error of the LCAO bands with respect to the PW reference bands (in eV) is given for the valence bands (σ_v) and the first two conduction bands (σ_c). The superscript v means 'optimized for the valence band'. The STO 2-z bases are after [21].

	Basis		$\mathcal{S}_Q$	$\mathcal{S}_{8(4)}$	σ_v	σ_c
Si	$\mathrm{STO3}^v$	sp	0.0074	0.1548	0.29	1.95
	STO	2-z	0.0099	0.0735	0.36	1.50
	$\mathrm{STO3}^v$	spd	0.0009	0.0101	0.09	0.23
	$\mathrm{PAO}_{5.0}$	sp	0.0139	0.1591	0.36	2.09
	$\mathrm{PAO}_{5.0}$	2-z	0.0085	0.0827	0.36	1.50
	$\mathrm{PAO}_{5.0}$	spd	0.0042	0.0132	0.15	0.38
C	$\mathrm{STO3}^v$	sp	0.0024	0.0790	0.17	3.36
	STO	2-z	0.0032	0.0059	0.36	0.40
	$\mathrm{PAO}_{4.0}$	sp	0.0041	0.0672	0.23	2.22
	$\mathrm{PAO}_{4.0}$	2-z	0.0018	0.0165	0.28	1.37

$\mathcal{S}_4$ for Al). It can be seen how an improvement in $\mathcal{S}_{8(4)}$ is accomplished when optimizing the basis for it—but the price being paid in the worsening of $\mathcal{S}_Q$. In addition to the $\mathcal{S}$- and σ-values, the band-gap region description is evaluated by showing the values of the Γ direct and indirect gaps, and the position of the minimum of the conduction band. An important and systematic improvement is observed in these quantities when the optimization is extended to unoccupied states. The information displayed offers the necessary information for the evaluation of the trade-off in the quality of the different spectral regions for the choice of a basis for a particular application. Figure 7 shows the band structure of Si obtained with a minimal sp STO3 basis optimized considering $\mathcal{S}_8$. Notice the nice agreement in the band-gap region, showing a very realistic indirect gap, quite rare for a minimal basis (compare with the typical cases shown in figures 8(a) and 8(d)). The LCAO bands have been shifted by 1.04 eV, which means an important deviation in total energies, if computed. Another price to pay is the very-long-range interactions due to the unusual extension acquired by the orbitals in the optimization.

Trying to improve the performance, other, more complicated, kinds of basis have also

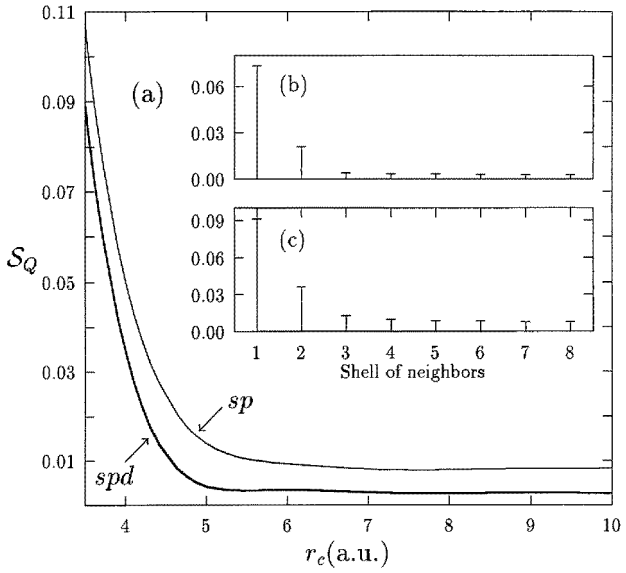

Figure 4. (a) Charge spillage for silicon with a PAO$_{r_c}$ sp and spd basis versus r_c; (b) charge spillage versus the shell of neighbours with non-zero overlaps for the spd basis; and (c) as (b), but for the sp basis.

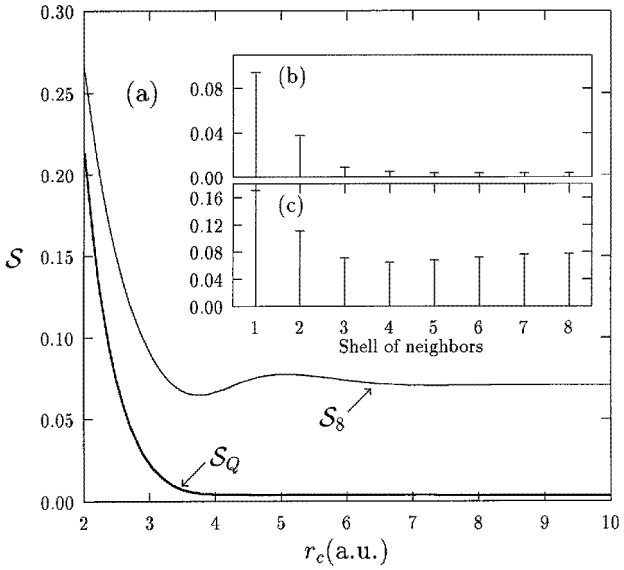

Figure 5. (a) Spillage for the occupied and first eight bands for diamond with a PAO$_{r_c}$ sp basis versus r_c; (b) charge spillage versus the shell of neighbours with a non-zero-overlaps basis; and (c) the same, but for the spillage of the first eight bands.

been tried, the results not being shown in the tables. Pseudo-STO (see section 4) provide good bases, but the improvements on the others (STO and PAO) have not been substantial

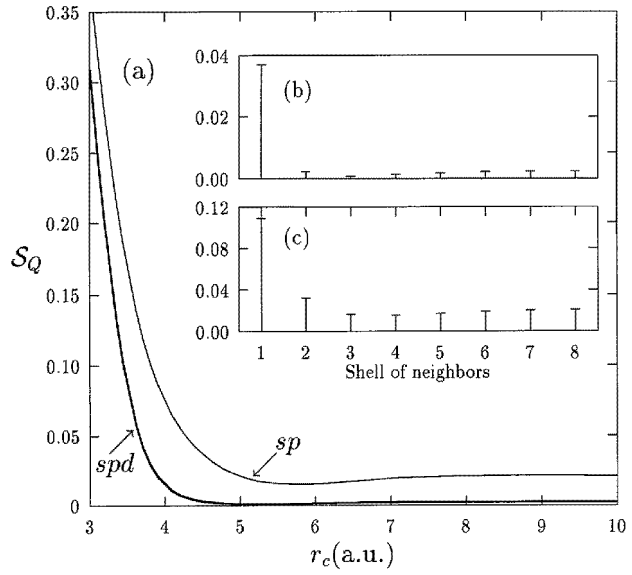

Figure 6. As figure 4, but for aluminium.

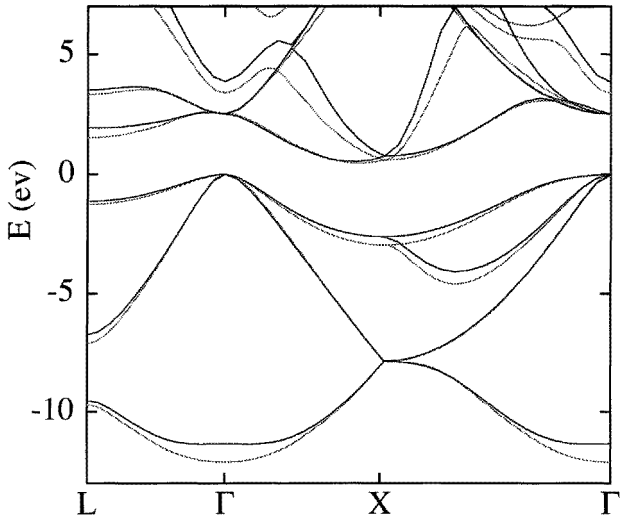

Figure 7. Gap optimization with a minimal basis. The silicon band structure calculated with a STO3 sp basis optimized to reproduce the occupied eigenstates and the first four conduction bands. The PW band structure is shown with dots. The STO3 bands have been shifted by 1.04 eV to make the tops of the two valence bands coincide.

enough for seriously considering them as alternative candidates. They have been optimized by varying the STO parameters outside of the core region (as for STO3) plus the extra degree of freedom given by the core radius. For Si a minimum in $\mathcal{S}_Q$ is obtained for a core radius of 1 au, but the spillage is only 4% lower than the spillage of the STO3 case. This fact indicates that the projection is not so sensitive to the core regions as to worsen the overall

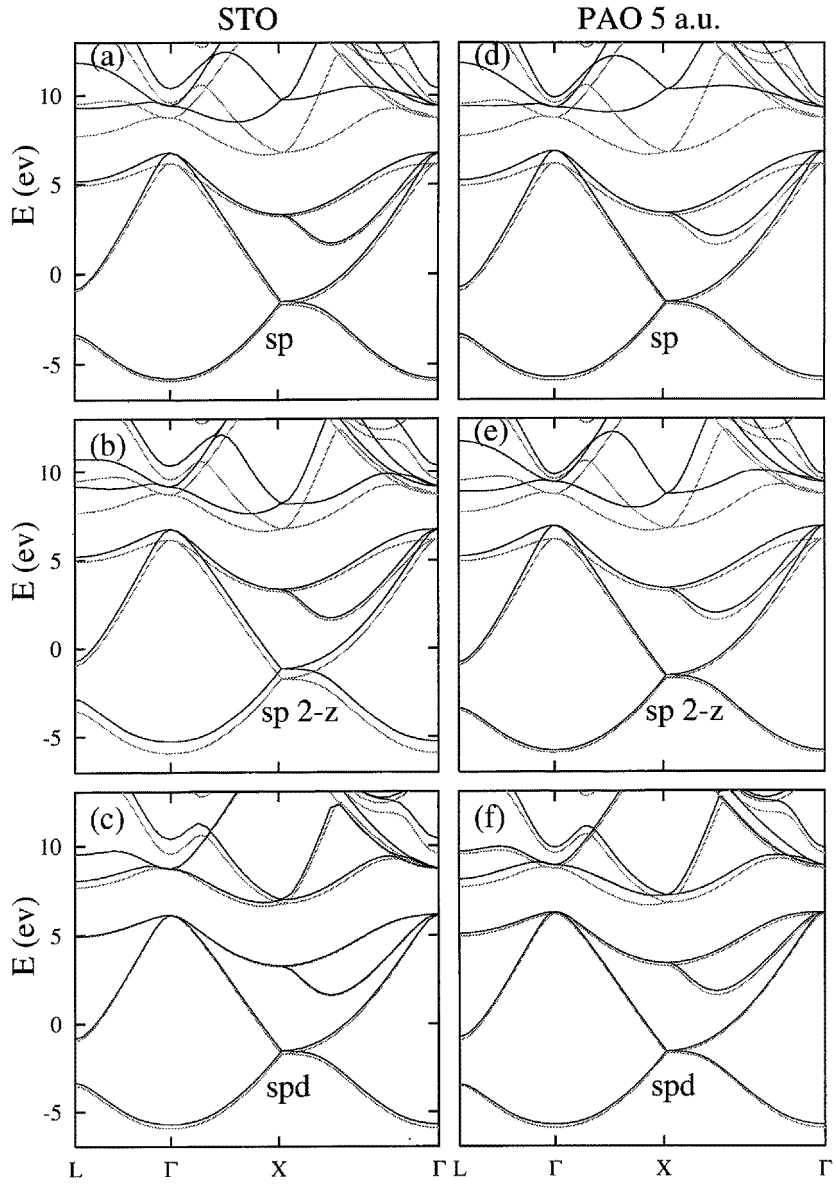

Figure 8. The band structure of Si for minimal, double-z, and spd bases. In (a), (b) and (c) the Hamiltonian is projected onto a STO3 sp, STO double-z, and STO3 spd basis, respectively. The STO3 bases are optimized for the valence band. (d), (e) and (f) correspond to $PAO_{5.0}$ sp, double-z, and spd bases. The PW reference band structure is shown with dots.

projection if the core region in the basis orbitals is not adapted to the pseudopotential.

Another kind of basis has been constructed based on PAO_{r_c}. More degrees of freedom are given to the spillage minimization by linearly combining excited states of the atomic problem with the ground state. For each symmetry (s, p_x, p_y, p_z, ...) the atomic orbital is constructed with a linear combination of the ground and excited states of the corresponding

pseudopotential. This procedure considerably reduces the spillage without increasing the size of the basis. However, the band-structure features are not accordingly improved. This fact leads to the conclusion that, for the spillage–energy correlation to be satisfactory in the solid, the energetics in the basis itself (in the atomic problem) has to be considered.

6.2. The range of interactions

An important aspect defining the applicability of LCAO bases is their range of interactions, i.e., the scope of neighbour shells that have to be included in the LCAO Hamiltonian and overlap matrices. The basis sets giving comparable results in the previously shown quantities perform quite differently in this respect. This is shown in table 3. This information is obtained by computing the atomic matrix elements of the Hamiltonian and overlap matrices as described in section 2. Due to the different analytical expressions for the orbitals, to measure the interaction range we adopt an 'empirical criterion', namely, the radius $r_{99.9\%}$ for which 99.9% of the norm of the orbital is within the sphere with that radius. We have found that this criterion is meaningful in the sense that neglecting interactions beyond that radius does not appreciably alter the energy bands corresponding to the valence and some conduction bands (average error lower than 0.05 eV). Neglecting interactions within this radius produces appreciable deviations in the bands. For PAO_{r_c} the interacting scope is clearly defined by r_c (which includes 100% if the norm is within), but for short r_c they are very similar to $r_{99.9\%}$, and for larger r_c then $r_{99.9\%}$ becomes more meaningful. Therefore, we also characterize the PAO_{r_c} with $r_{99.9\%}$. Besides this quantity, table 3 also shows the scope of non-negligible neighbouring shells for each case.

PAO_∞ represents the best basis as far as spillage and band quality are concerned, and also for population purposes [9] (see the next section), but its range of interactions is very large. This fact was already pointed out by Jansen and Sankey [14] in their work on self-consistent calculations using this basis. The results of our calculations show that interactions up to at least five (ten) shells of neighbours have to be retained for Si (C) to obtain a reasonable band structure with the correct semiconducting behaviour. The best basis suited for a shorter range of interactions, together with keeping good standards in spillage and band structure, is the PAO_{r_c}, as can be seen in table 3 and figure 4 for Si, in figure 5 for C, and in figure 6 for Al. Note that, in spite of C needing a smaller r_c than Si to attain small spillages, the range of neighbours is larger for C due to the much smaller lattice parameter.

6.3. Polarized and double-z basis sets

The clearest way of improving the quality of a basis is increasing its size. In LCAO there are two usual ways of doing this: (i) increasing the number of orbitals within the same atomic symmetries as found in the minimal basis; and (ii) polarizing the basis. Within the first, the double-z case is the most usual one, i.e., doubling the basis, which in the cases of this paper means a basis of two s, two p_x, two p_y and two p_z orbitals. A polarization of the basis is accomplished when a shell of different atomic symmetry is added to the minimal basis. In our cases this means the addition of the d shell to the minimal sp basis. Combination of these two procedures is also customary for further improvement. A rule of thumb in quantum chemistry says that a basis should always be doubled before being polarized [5]. This is not the usual practice within the LCAO calculations in the solid-state-physics community, where double-z bases are hardly to be found.

Expanded STO bases can be found in the literature [5]. This is not the case for PAO.

In this paper we propose to use the excited states of the atomic calculations leading to the PAO_{r_c}, under the same boundary conditions, to obtain the orbitals required to expand the basis, i.e., excited s and p orbitals for double-z bases and d orbitals for polarization. The advantages of this scheme are its simplicity and the controlled range of interactions for the added orbitals also, which is usually lost in the traditional scheme.

Again, we study here the quality of expanded LCAO bases by means of their spillage and their band structure as obtained from the projection. The results of our analysis are shown in table 4, where minimal (single-z), double-z, and polarized single-z bases are compared for silicon and diamond. See also table 1 for aluminium. The sp and spd bases are optimized as above using STO3 for the Slater orbitals, and using the corresponding r_c for the PAO, as shown in figures 4–6. The double-z basis for STO has been taken from the literature [5, 21]. Note that, with the double-z basis, Si does not reach equivalent quality to C, and that, for that purpose, the polarization of the basis is quite enough.

Table 5. The band gap in Si and C (diamond) for single-z and double-z (2-z) bases. E^{Γ}_{gap} and E_{gap} stand for the direct-gap energy at Γ and for the absolute gap energy, respectively, both in eV. $\boldsymbol{k}$ is the wave vector of the minimum of the conduction band in units of π/a, being $|\boldsymbol{k}| = 1$ for the X point.

	Basis		E^{Γ}_{gap}	E_{gap}	$\lvert\boldsymbol{k}\rvert$
Si	$STO3^v$	sp	2.65	1.74	0.60
	STO	2-z	2.40	0.88	0.73
	$STO3^v$	spd	2.58	0.76	0.85
	$PAO_{5.0}$	sp	2.47	2.18	0.47
	$PAO_{5.0}$	2-z	2.49	1.03	0.70
	$PAO_{5.0}$	spd	2.65	0.91	0.85
	PW		2.55	0.45	0.85
C	$STO3^v$	sp	6.32	6.18	0.41
	STO	2-z	5.46	4.30	0.73
	$PAO_{4.0}$	sp	5.98	5.89	0.34
	$PAO_{4.0}$	2-z	6.00	5.28	0.53
	PW		5.28	3.43	0.76

The band structures corresponding to the data of table 4 are shown in figure 8 for Si, figure 9 for C, and figure 10 for Al (table 1), in each case comparing the LCAO bands obtained from the projection with the reference PW bands. The information given in the table is ratified, and observed in more detail. Note that the substantial improvement in the Si case occurs when including the d orbitals, but not when doubling the minimal basis. For diamond, however, such qualitative improvement is given by the double-z basis. The figures for the gap in the Si and C cases are shown in table 5. In the Al case, the polarization is needed from the start, the sp projection giving defective band structures in the neighbourhood of the Fermi level around the W point. The spd band structure is shown in figure 10 for PAO_{r_c} for different r_c. The performance of the double and polarized STO bases in the first conduction bands is better than that of the corresponding PAO_{r_c} bases. This is due to the larger extension of the extra orbitals in the STO bases, which is not allowed in the PAO_{r_c}. The latter, however, also represent a considerable improvement over the minimal bases,

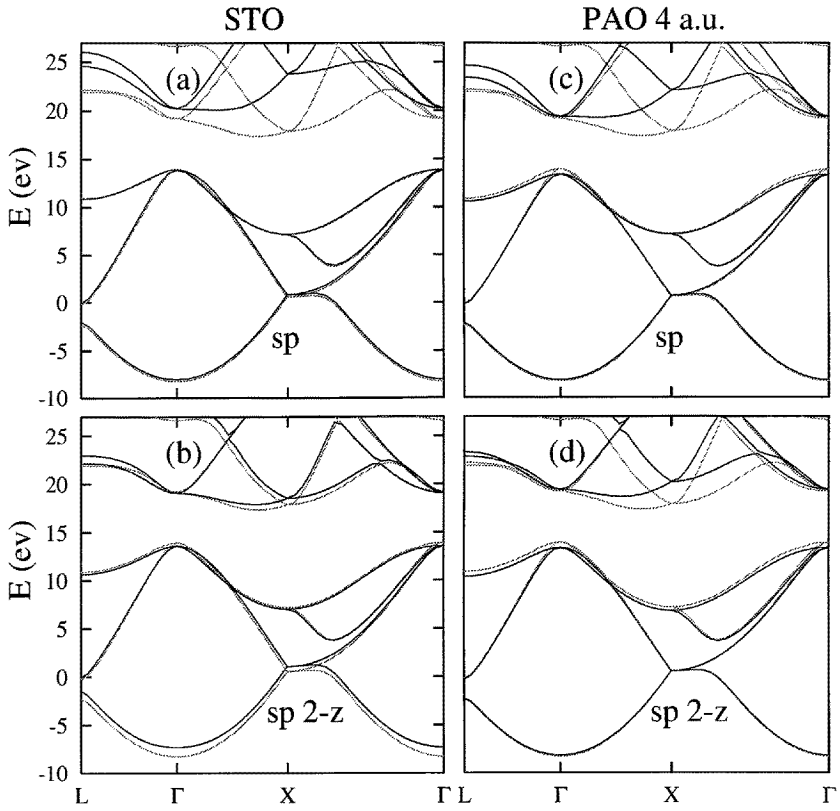

Figure 9. The band structure of diamond for single-z and double-z bases. (a) and (b) correspond to the projection onto a STO3 sp and STO double-z basis set, respectively. The STO3 basis is optimized for the valence band. (c) and (d) correspond to $PAO_{4.0}$ sp and double-z bases. The PW reference band structure is shown with dots.

while keeping the interaction range. This virtue makes them very appealing for accurate LCAO calculations.

The error in the band structures could be noticeably reduced with a rigid shift of the bands, which is clear in view of the figures. This has not been allowed, in order to keep the band-structure error as representative of the behaviour to be expected of total energies.

6.4. Geometry and environment dependence

The projection procedure proposed in this paper is based on PW calculations of actual materials. As compared to basis optimization in atoms, this allows equating the basis to particular environments or geometries. As a first example we show the change in the minimal sp PAO_{r_c} basis for C depending on the solid being diamond or graphite. Figure 11 shows the charge spillage as a function of r_c and of the range of interacting neighbouring shells. Graphite is less well represented by the same kind of basis. In addition, graphite requires a larger r_c to approach minimum spillage. This latter fact is due to the comparatively large interplanar distances in the graphite structure.

Another example of geometry dependence of the basis quality is given in figure 12,

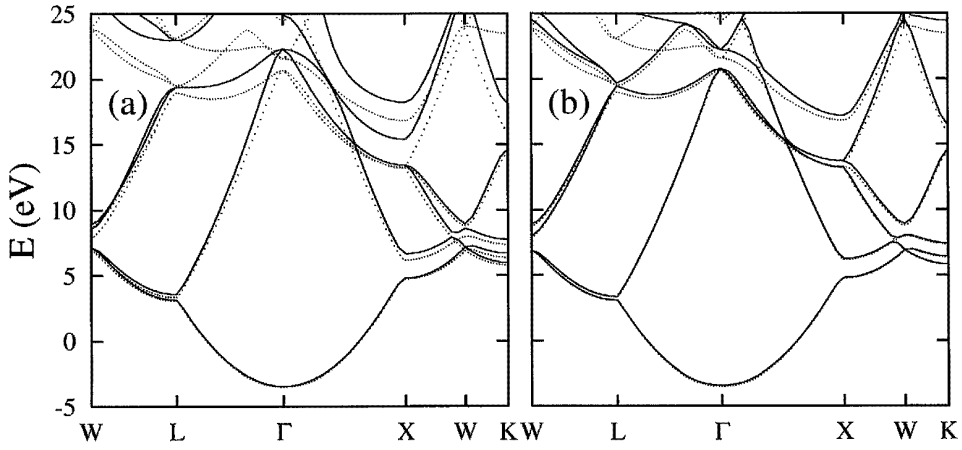

Figure 10. The aluminium band structure: (a) calculated with the $PAO_{5.3}$ spd basis; and (b) calculated using the $PAO_{6.1}$ basis. Dotted lines show the PW band structure (the Fermi energy is 8.2 eV).

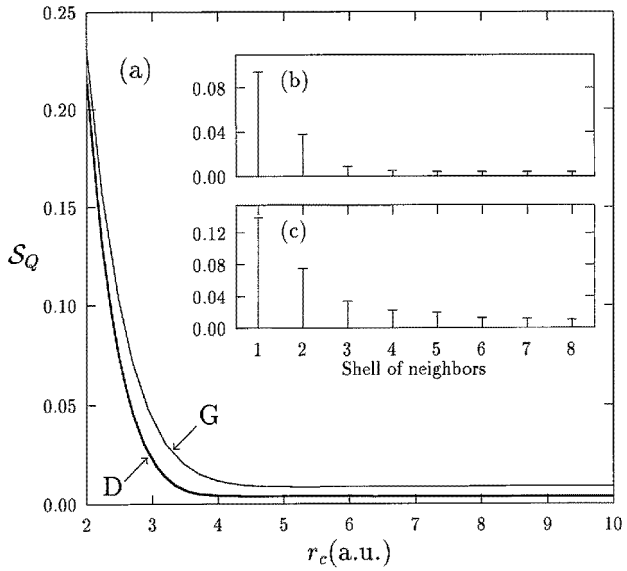

Figure 11. (a) Charge spillage for diamond (D) and graphite (G) as a function of r_c for a PAO_{r_c} sp basis. (b) Charge spillage for diamond as a function of the shell of neighbours with non-zero overlap, and (c) the same for graphite.

where the charge spillage of a minimal PAO_{r_c} for Si is plotted versus the lattice constant for different values of r_c. From the figure it is clear that (i) for spillage purposes and, therefore, for the total energy, the basis is better the larger r_c, (ii) the slope in $\mathcal{S}_Q$ versus lattice constant will translate to a corresponding slope of the total energy, which gives rise to a fictitious pressure on the system, (iii) this pressure differs according to the value of r_c, and the optimum r_c for this purpose (the one giving zero pressure, with r_c between 5 and

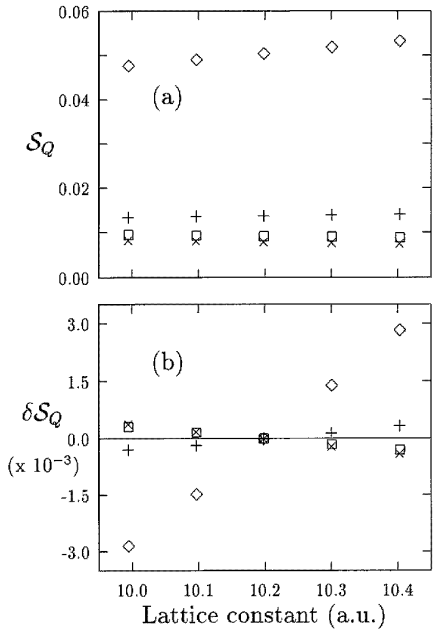

Figure 12. (a) $\mathcal{S}_Q$ versus the lattice constant of silicon for PAO_{r_c} bases, (b) $\delta\mathcal{S}_Q = \mathcal{S}_Q - \mathcal{S}_Q^{eq}$ where the $\mathcal{S}_Q^{eq}$ is taken at the equilibrium value of the lattice constant $a_0 = 10.2$ au. $\Diamond$ stands for $r_c = 4$ au, $+$ for $r_c = 5$ au, $\Box$ for $r_c = 6$ au, and $\times$ for $r_c = \infty$.

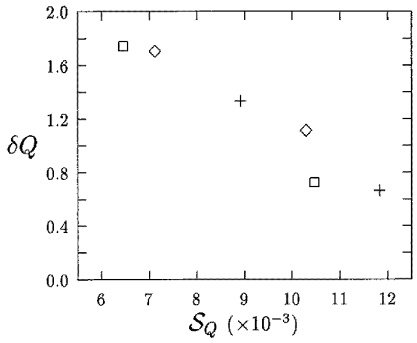

Figure 13. The charge transfer in SiC as a function of the charge spillage of the sp basis used to project the density. $\Box$ stands for PAO_∞ optimized for the heteropolar system and independently for Si and C in a zinc-blende structure; $\Diamond$ stands for the STO3 basis in the same conditions; and $+$ stands for a STO2 basis.

6 au) is different from the optimum for energy considerations ($r_c = \infty$), and (iv) there are no appreciable curvatures, from which it can be inferred that no substantial deviations are to be expected in the elastic and force constants (vibrations) due to the basis.

7. Population analysis

One of the uses of the projection into a LCAO is the possibility of performing population analysis of the PW results, which is otherwise inaccessible. It is well known that any population analysis has an inherent arbitrariness associated with the fact that the relevant quantities in the analysis do not correspond to observables, but rather to convenient ways of dissecting the total charge of the system. Furthermore, small variations in the basis can produce quite different population results, particularly for charge transfers. In spite of this, much of the chemical description of condensed systems is performed in the language given by such population analyses. We, therefore, consider it worthwhile to explore this problem with the spillage.

Due to the above-mentioned arbitrariness, the correlation of charge transfers and charge spillage is expected to be poor. This is clear when the basis is made uncompensated—like, for instance, when introducing d orbitals for silicon in SiC. This greatly improves the description of the eigenfunctions and reduces the spillage, but as the basis is uncompensated, some features (the structure of the bond) are described by the much more complete basis of one of the atoms, so more electronic charge is assigned to the atom with the more complete

basis, leading to an unphysical charge transfer. A compensated basis is therefore important for the populations to be meaningful. A measure of this compensation can be obtained if the spillage is calculated independently for structurally similar solids containing the individual atoms separately. The spillages for silicon and diamond separately, using the same kind of basis for the two, indicate a slight lack of compensation favouring diamond, which, in this case, indicates that the charge transfer might be slightly overestimated. In addition to that, the optimization of the basis is important for obtaining reliable values of charge transfers. This is seen in figure 13, where the charge transfer in SiC is shown to correlate with the spillage. A 'converged' charge transfer is not guaranteed, but, provided that the basis is compensated, a small spillage indicates a meaningful charge transfer.

Table 6. Calculated excess charge, in units of e, for the upper and lower Si atoms in the dimer of a Si(100)–2×1 surface. A minimal sp basis has been used in all cases. $\mathcal{S}_Q$ stands for the charge spillage. $\mathrm{PAO}_\infty^{opt}$ and STO1 have been optimized for bulk silicon. $\mathrm{STO1}_{1.75}$ is a STO1 basis with $\beta = 1.75$ au^{-1} [5].

Basis	$\mathcal{S}_Q$	δQ_{up}	δQ_{down}
PAO_∞	0.0080	-0.10	$+0.12$
$\mathrm{PAO}_\infty^{opt}$	0.0078	-0.10	$+0.13$
$\mathrm{PAO}_{5.0}$	0.0139	-0.13	$+0.10$
$\mathrm{STO1}_{1.75}$	0.0318	-0.15	$+0.10$
STO1	0.0076	-0.13	$+0.12$

The charge transfers for some zinc-blende semiconductors (BN, BP, AlP, SiC, and GaAs) obtained with the projection procedure using optimized PAO_∞ basis sets are shown in table 1 of [9]. The numbers compare well with equivalent results obtained from direct LCAO self-consistent calculations [22, 23]. Systems with only one species do not present these difficulties for the charges since the basis can be trivially compensated. Table 6 shows the excess of charge (with respect to the neutral atom) assigned to the upper and lower atoms of a dimer in the Si(100)–2×1 surface [24]. A minimal basis has been used. The populations are quite stable and independent of the basis used.

8. Conclusions

We have presented a projection method which provides a tool for characterizing and optimizing atomic orbital basis sets for a given system. Independently of how many bases are evaluated for that particular system, only *one* reference self-consistent plane-wave calculation is required. The method also provides LCAO band structures, Hamiltonian matrix elements (non-fitted tight-binding parameters), and population analysis.

Based on that tool and on its characteristic parameter, the spillage, an exhaustive analysis of two kinds of LCAO basis set, namely, Slater-type (STO) and pseudo-atomic (PAO) orbitals, has been presented for several solids, arriving at the following conclusions.

(i) The spillage provides a very convenient tool for studying and variationally optimizing basis sets, that closely correlates with energy optimizations.

(ii) The LCAO band structures obtained from the projection allow one to characterize separately the errors due to the incompleteness of the basis and to considering a limited range of interactions. This is due to the fact that the bands are obtained directly in Bloch space, with interactions to infinite neighbours.

(iii) Both STO and PAO optimized with spillage minimization give quite good basis sets, of comparable quality.

(iv) If a controlled range of neighbour interactions is desired, the best-performing basis sets are provided by the PAO_{r_c} introduced by Sankey and Niklewski [13].

(v) A simple and interaction-range-controlled scheme for extending PAO basis sets to double-z and/or polarized bases is proposed, and shown to give good basis sets.

(vi) Double-z bases substantially improve the performance for diamond, whereas d polarization is required for similar results for Si and Al.

(vii) The spillage minimization allows optimization tailored for particular uses, e.g. the description of excitations or band gaps, and environmental dependence of the basis.

(viii) Population analysis can be performed, and its intrinsic arbitrariness can be partially controlled by means of the spillage.

Acknowledgments

We acknowledge useful discussions with F Ynduráin and P Ordejón. This work was supported by the Dirección General de Investigación Científica y Tecnológica of Spain (DGICYT) under grant PB92-0169.

References

[1] Eschrig H 1987 *Optimized LCAO Methods* (Berlin: Springer) and references therein
[2] See, for instance,
Ihm J, Zunger A and Cohen M L 1979 *J. Phys. C: Solid State Phys.* **12** 4409
[3] Hamann D R, Schlüter M and Chiang C 1979 *Phys. Rev. Lett.* **43** 1494
[4] Ordejón P, Drabold D A, Martin R M and Grumbach M P 1995 *Phys. Rev.* B **51** 1456 and references therein
[5] Poirier R, Kari R and Csizmadia I G 1985 *Handbook of Gaussian Basis Sets* (Amsterdam: Elsevier Science) and references therein
[6] Chadi D J 1977 *Phys. Rev.* B **16** 3572
[7] Francisco E, Seijo L and Pueyo L 1986 *J. Solid State Chem.* **63** 391 and references therein
[8] García de la Vega J M, Fernández Rico J and Fernández-Alonso J I 1990 *J. Mol. Struct. (Theochem.)* **210** 79
[9] Sánchez-Portal D, Artacho E and Soler J M 1995 *Solid State Commun.* **95** 685
[10] Ordejón P and Ynduráin F 1991 *Phys. Rev.* B **43** 4552
[11] Artacho E and Ynduráin F 1991 *Phys. Rev.* B **44** 6169
[12] Artacho E and Miláns del Bosch L 1991 *Phys. Rev.* A **43** 5770
[13] Sankey O F and Niklewski D J 1989 *Phys. Rev.* B **40** 3979
[14] Jansen R W and Sankey O F 1987 *Phys. Rev.* B **36** 6520
[15] Monkhorst H J and Pack J D 1976 *Phys. Rev.* **13** 5188
[16] Moreno J and Soler J M 1992 *Phys. Rev.* B **45** 13 891
[17] Mulliken R S 1955 *J. Chem. Phys.* **23** 1833
[18] Troullier N and Martins J L 1991 *Phys. Rev.* B **43** 1993
[19] Hohenberg P and Kohn W 1964 *Phys. Rev.* **136** B864
Kohn W and Sham L J 1965 *Phys. Rev.* **140** A1133
[20] Kleinman L and Bylander D M 1982 *Phys. Rev. Lett.* **48** 1425
[21] Ordejón P, private communication
Basis 14-20-1 from [5] slightly modified for bulk calculations has been used for Si and a contraction of the basis proposed by
van Duijneveldt 1971 *IBM J. Res. Rep.* RJ945
has been used for diamond.
[22] Orlando R, Dovesi R, Roetti C and Saunders V R 1990 *J. Phys.: Condens. Matter* **2** 7769
[23] Chelikovsky J R and Burdett J K 1986 *Phys. Rev. Lett.* **56** 961
[24] Geometry taken from
Soler J M, unpublished